RSER

# Materials and system requirements of high temperature thermal energy storage systems: A review. Part 2: Thermal conductivity enhancement techniques.

Jaume Gasia, Laia Miró, Luisa F. Cabeza*

GREA Innovació concurrent, Edifici CREA, Universitat de Lleida, Pere de Cabrera s/n, 25001-Lleida (Spain).

* Corresponding author: Phone: +34-973-003576, fax: +34-973-003575, e-mail: lcabeza@diei.udl.cat

**Abstract**

This review is focused on the study of the requirement of high thermal conductivity of thermal energy storage (TES) materials and the techniques used to enhance it as this is one of the main obstacles to achieve full deployment of TES systems. Numerical and experimental studies involving different thermal conductivity enhancement techniques at high temperature (> 150 ºC) are reviewed and classified. This article complements Part 1, which reviews the different requirements that TES materials and systems should consider for being used for high temperature purposes and the approaches to satisfy them. The enhancements identified for this temperature range are the addition of extended surfaces like fins or heat pipes and the combination of highly conductive materials with TES material like graphite or metal foam composites and nanomaterials. Moreover the techniques presented are classified and discussed taking into account their research evolution in terms of maturity and publications.

**Key-words:** Thermal energy storage, High temperature, Thermal enhancement techniques, Thermal conductivity, Nanoparticles, Technology Readiness Level.

# 1. Introduction

Part 1 of this review [1] lists more than 25 different requirements that thermal energy storage (TES) materials (both sensible and latent) and TES systems should consider for being used for high temperature purposes (> 150 ºC) and it analyses the different literature approaches presented in previous studies to achieve such requirements. These requirements have been classified into chemical, kinetic, physical and thermal for the material point of view; and environmental, economic and technologic for the system point of view. Within all the requirements listed, this second part of the review is focused on the study of the requirement for high thermal conductivity of TES materials, being the one that has drawn more attention in the scientific community, and the techniques used to enhance their usually low values.

In a TES system, thermal energy needs to be transferred in the first place from an outer energy source to the TES material to be later on transferred from the TES material to an outer application. This transition needs to be done within a specific period of time and under different heat transfer mechanisms: conduction, convection or both. For instance, in a latent charging process, the TES material undergoes phase change as the heat transfer fluid (HTF) transfers heat to it, causing the melting front to move away from the heat transfer surface and, as a consequence, the solid layer of the material decreases while the thickness of the liquid layer increases. During all the process conduction is present. However, the higher presence of liquid state leads a higher presence of density gradients, which added to the fact that the thermal conductivity is lower in the liquid state than in the solid state, causes the convection to become dominant and the conduction negligible [2]. During the latent discharging process, or solidification, conduction becomes the dominant heat transfer mechanism since a layer of solid material is created at the very beginning around the heat transfer surface, reducing the effect of convection to become almost negligible. Therefore, materials with low thermal conductivity coefficients, which mean high thermal resistance and slow charging and discharging rates, drastically decrease the thermal performance of TES and limit possible large-scale applications.

It is a fact that most of the commercial TES materials that are currently available at the market have intolerably low thermal conductivity values (0.2–1 W/(m·K)), allowing the researchers to try to make up for such poor values by proposing heat transfer enhancement techniques, not only for improving the TES material itself but also for improving the effective thermal conductivity between the HTF and the TES material, which in some cases turn to be the same material.

Before introducing any external enhancer to the TES system, the researchers have to bear in mind in which physical state the TES material is going to be used, whether the liquid phase, the solid phase or both, since their introduction can enhance the thermal performance of one state but can decrease the thermal performance of the other state. Hence, a previous study or discussion should be done in order to know the advantages and disadvantages of the thermal conductivity enhancement technique which is desired to be used.

The aim of the present study is to review the thermal conductivity enhancement techniques used in high temperature TES systems and materials for both enhancing the effective thermal conductivity between the HTF and the TES material by adding extended surfaces, and enhancing the thermal conductivity of the material itself by combining it with highly conductive materials (Fig. 1).

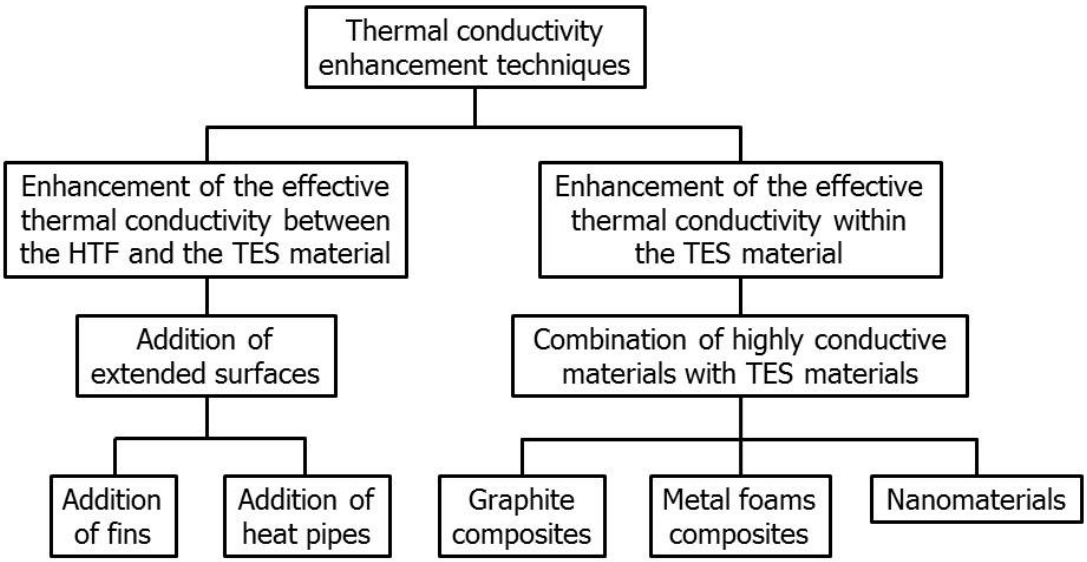


Fig. 1. Thermal conductivity enhancement techniques for high temperature purposes.

## 2. Addition of extended surfaces

The most and widely studied thermal conductivity enhancement technique in the different temperature ranges is the extended surfaces. This technique consists of increasing the heat transfer surface between the HTF and the TES material by arranging fins or heated pipes on the HTF tubes embedded in the TES system. This technique leads to an increase of the effective thermal conductivity as it diminishes the distance between the storage material and the HTF, and reduces the thermal resistance between the HTF and the TES material. However, two main drawbacks are associated to this technique: on the one hand the increase of costs due to the increase of the extended surfaces material and on the other hand the decreasing of the packing

factor of the TES system, which is the ratio that defines the percentage of volume of TES material in front of the total volume of the storage container, due to the increase of the volume occupied by the extended surfaces.

Despite the fact that not many experimentation at high temperature has been carried out, the criteria that should be borne in mind when designing a TES system with the extended surfaces enhancement technique is the same than the used at lower temperatures: HTF pipe dimensions, material of the extended surfaces, geometry of the extended surfaces, arrangement of the extended surfaces, good interaction between the TES material, the HTF and the material of the extended surfaces and finally the boundary conditions of the TES system.

The two main enhancement techniques regarding the extended surfaces which have been studied by different researchers are the addition of fins and the addition of heated pipes.

## 2.1 Addition of fins

Concerning to the addition of fins, first references lead us to Zhang et al. [3] who numerically studied the heat transfer enhancement in a latent heat TES (LHTES) system by using an internally finned tube. A comparison with a plain tube, in terms of the melting volume factor, was performed, concluding that this factor could be significantly increased by increasing the thickness, height and number of fins for a HTF with low thermal conductivity and low Reynolds numbers.

Seeniraj et al. [4] numerically studied the improvement in terms of temperature, melting front location and thermal energy stored of an externally finned tube in a space based LHTES unit for solar dynamic power generation. An enhancement of the performance by increasing the number of fins for a given set of geometrical parameters and depending on the thermophysical properties of the tube material and the HTF-TES material combination was observed.

Khaled [5] numerically proposed a variation of the fin enhancement technique called *hairy fin system,* which consists of a primary rectangular fin with a large number of slender secondary rods attached on its surface (Fig. 2). This technique increased the heat transfer, if compared to a rectangular fin, with low secondary fins diameter and high secondary thermal conductivity.

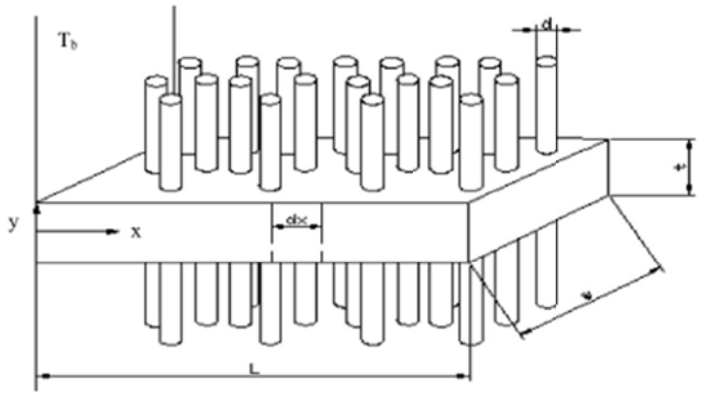


Fig. 2. Schematic diagram of the hairy fin system [5].

Guo and Zhang [6], Jung and Boo [7] and Tiari et al. [8] numerically studied how the addition of aluminum fins and the variation of different geometric and thermal parameters affected the heat transfer enhancement during the discharging process in a LHTES. Results showed that the magnitude of the enhancement was dependent on the geometry of the fins, fins spacing, HTF tube radius, boundary conditions and thermal conductivity values of the TES material.

The German Aerospace Center (DLR) theoretically proposed and experimentally developed different designs concerning both embedded and finned tubes enhancement techniques, for solar thermal power generation and high temperature process heat [9][10][11]. Eutectic mixtures of $KNO_3$, $NaNO_2$ and $NaNO_3$ were selected as base materials and materials such as graphite, aluminum, stainless steel and carbon steel were considered for fins. Results showed that a decreasing on the number of tubes could be achieved if the thermal conductivity of the TES material was increased and a reduction of the charging process time if graphite was used as fin material for applications up to 250 °C and aluminum for higher temperatures applications (Fig. 3).

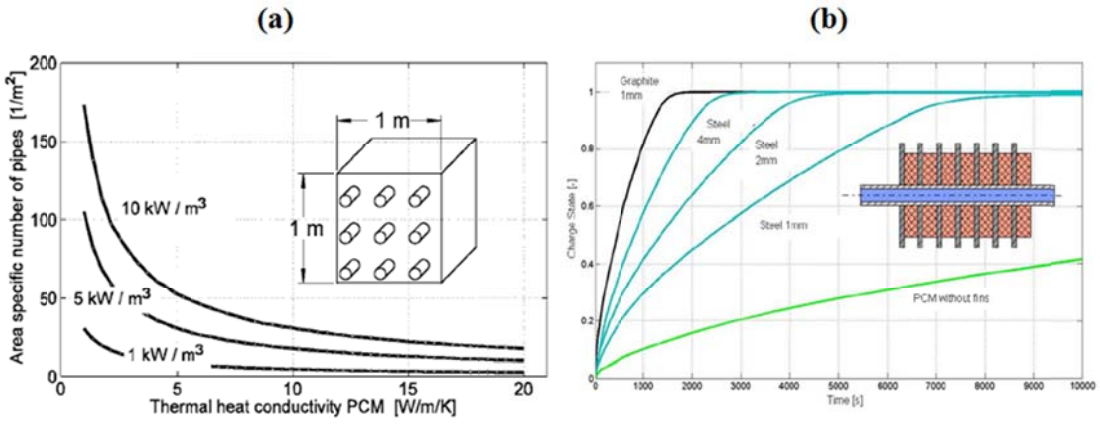


Fig. 3. (a) Effect of thermal conductivity on the number of required pipes [10]. (b) Effect of material fins on the process of charging [11].

Tao et al. [12] numerically studied the behavior of three geometrically different fins enhancement techniques (dimpled, cone-fined and helically-fined) in terms of TES material melting rate, solid–liquid interface, TES capacity, TES efficiency and HTF outlet temperature for a dish solar thermal power generation system. Results showed that all three enhanced tubes could effectively improve the thermal performance of the system, being the helically-finned tube the one with better results (Fig. 4).

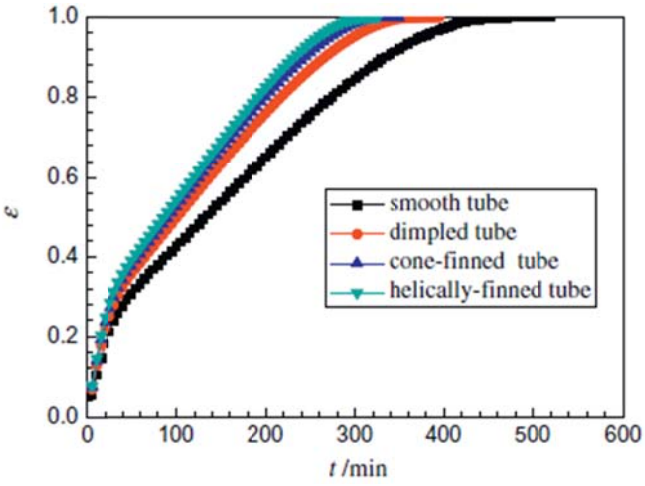


Fig. 4. Effects of the fins enhancement techniques on the heat storage efficiency [12].

Gil et al. [13] developed an experimental study at pilot plant scale with a finned shell-and-tubes heat exchanger. It consisted of a high temperature TES system for solar cooling applications and analyzed two similar storage tanks based on shell-and-tubes heat exchanger configuration with the only difference that one of them incorporated 196 squared fins on the tubes bundle. Results showed a decrease in the melting/solidification periods and higher heat transfer rates for partial charging and discharging processes in the tank with fins.


Fig. 5. (a) Storage TES system without fins. (b) Storage TES system with fins used in the experimentation [13].

## 2.2 Addition of heat pipes

Embedded heat pipes, also referred in different studies as thermosyphons, are gaining relevance as a heat transfer enhancement technique due to their high effective thermal conductivity that facilitates the heat transfer from the TES material to the HTF and vice versa. This system consists of several small closed tubes which are attached to the main pipe and whose inside is filled with a working fluid which undergo liquid-vapor phase change at the ends of such heat pipes, called evaporator and condenser sections. That allows the thermal performance enhancement in the heat transfer (Fig. 6).

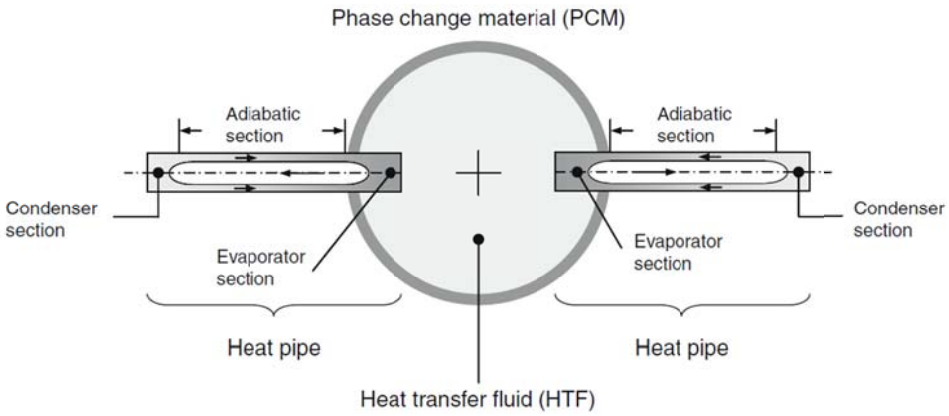


Fig. 6. Embedded heat pipe scheme [14].

Regarding this technique, only numerical studies have been performed [15][14][16][17] [18] [19]. Shabgard et al. [14] and Nithyanandam and Pitchumani [16][17] developed a thermal network model to analyze a heat transfer in a high temperature LHTES unit with different arrangements of embedded heat pipes for solar thermal electricity generation evaluating the effect of HTF flow direction and the number of heated pipes among others (Fig. 7). Results showed a reduction of the thermal resistance of the unit as well as well as a relation between the effectiveness of the heat pipes and the variation on several HTF parameters: higher HTF mass flow rate and tube diameter implied lower effectiveness of the heat pipes and vice versa. A similar study was carried out by Khalifa et al. [18], whose simulated results showed that the energy extracted after 4 h by a finned heat pipe was 86% higher than that of a bare one.

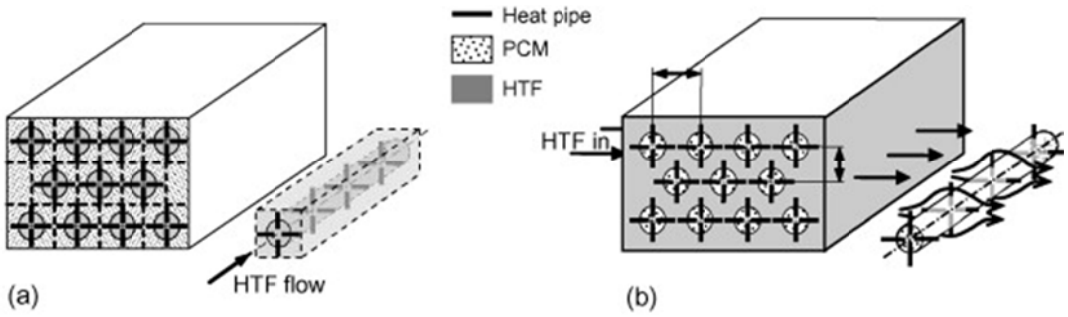


Fig. 7. Two LHTES units: (a) the TES material surrounds the HTF tubes, (b) the HTF passes over tubes containing TES material [14].

Finally, Robak et al. [19] theoretically and numerically studied, in economic terms, the incorporation of thermosyphons in a large scale LHTES system for commercial collector solar plants (CSP) and compared the results with a two-tank sensible heat TES (SHTES). Results showed the economic competitiveness of such system, with a reduction of 15% in the capital costs.

Table 1 and Table 2 review, in a chronological order, the different studies carried out at high temperature concerning the extended surfaces enhancement techniques, showing the enhancement technique used, the study case, the main characteristics of the TES system, the comparison performed and the improvement observed.

Table 1. Review of the studies concerning the extended surfaces techniques at high temperature in terms of thermal conductivity enhancement. Case 1: Addition of fins.

| Technique | | System geometry | Study case | TES material | Pipes/Fins material | HTF material | Comparison | Improvement | Year | Reference |
|---|---|---|---|---|---|---|---|---|---|---|
| 1 | Internally finned tube – Single longitudinal fin | Annular shell | Numerical | n.a. | n.a. | n.a. | Finned – plain tubed | Percentage of improvement depending on height and width of the fins | 1996 | Zhang and Faghri [3] |
| 2 | Externally finned tube – Multiple fins | Shell-and-tubes | Numerical | $LiF/MgF_2$ | n.a. | n.a. | Finned – plain tubed | Percentage of improvement depending on number of fins for a given set of geometrical parameters | 2002 | Seeniraj et al. [4] |
| 3 | Hairy fin system | Heated surface | Numerical | n.a | n.a. | n.a. | Hairy fins – Rectangular fins | Higher improvement if secondary fins diameter decreases | 2007 | Khaled [5] |
| 4 | Externally finned tube – Multiple fins | Shell-and-tubes | Numerical | $KNO_3/NaNO_3$ | Aluminium | n.a | Finned – plain tubed | Percentage of improvement depending on geometry of fins | 2008 | Guo and Zhang [6] |
| 5 | Finned tube | Shell-and-tubes | Theoretical | n.a | n.a | n.a | n.a | Reduction of number of pipes | 2008 | Tamme et al. [10] |
| 6 | Externally | Storage tank | Theoretical & | $KNO_3/NaNO_2/KaNO_3$ | Graphite | Thermal oil | Finned – plain | Depending on the | 2009 | Laing et al. |

| | | | | | | | | | | |
|---|---|---|---|---|---|---|---|---|---|---|
| | finned tube | | experimental | $KNO_3/NaNO_3$ $NaNO_3$ | Aluminum Stainless steel Carbon steel | Steam | tube | shape and materials of the fins | | [11] |
| 7 | Externally finned tube | Shell-and-tubes | Numerical | $LiF/CaF_2$ | n.a | He/Xe | Smooth (S) Dimpled (D) Cone-finned (CF) Helically-finned (HF) | Reduction on the melting time of 19.9% (D), 26.9 % (CF) and 30.7 % (HF) | 2012 | Tao et al. [12] |
| 8 | Externally finned tube – multiple fins | Shell-and-tubes | Experimental | Hydroquinone | Stainless steel | Therminol | Finned – plain tube | Charging/discharging time enhancement | 2014 | Gil et al. [13] |
| 9 | Externally finned tube | n.a. | Numerical | $KNO_3$ | Nickel | n.a. | Geometrical parameters | Percentage of improvement depending on number of fins and geometrical parameters | 2015 | Tiari et al. [8] |

*n.a*: not available

Table 2. Review of the studies concerning the extended surfaces techniques at high temperature in terms of thermal conductivity enhancement. Case 2: Addition of heat pipes.

| | Technique | System geometry | Study case | TES material | Pipes/Fins material | HTF material | Comparison | Improvement | Year | Reference |
|---|---|---|---|---|---|---|---|---|---|---|
| 1 | Embedded heat pipes | Shell-and-tubes | Numerical | $KNO_3$ | Stainless steel | Therminol | Distribution TES material/HTF and orientation of heat pipes | Depending on the influence of the number of heat pipes and HTF flow direction | 2010 | Shabgard and Bergman [14] |
| 2 | Embedded heat pipes | Shell-and-tubes | Numerical | $KNO_3$ | Stainless steel | Therminol | Orientation of heat pipes | Depending on HTF mass flow rate, module length, tube length of the condenser section, length of the evaporator section and the vapor core radius | 2011 | Nithyanandam and Pitchumani [16] |
| 3 | Embedded heat pipes | n.a. | Numerical | $NaNO_3$<br>$NaOH/NaCl/Na_2CO_3$<br>$KNO_3$<br>LiCl/KCl<br>KOH<br>$MgCl_2/KCl/NaCl$ | Carbon steel | Therminol<br>Diphenyl<br>Naphthalene<br>potassium | Sensible/Latent | 15% reduction in capital in latent over sensible | 2011 | Robak et al. [19] |
| 4 | Embedded heat pipes | Shell-and-tubes | Numerical | $KNO_3$ | Stainless steel | Therminol | Different arrangements | Higher effectiveness for 4 thermosyphons | 2013 | Nithyanandam and |

| | | | | | | | | | | |
|---|---|---|---|---|---|---|---|---|---|---|
| | | | | | | | of thermosyphons | | | Pitchumani [17] |
| 5 | Finned heat pipes | Shell-and-tubes | Numerical | n.a | n.a | n.a | Finned – plain tube | With 4 fins: energy extracted:86% at the same time heat pipes effectiveness: 24% | 2014 | Khalifa et al. [18] |
| 6 | Finned heat pipes | Shell-and-tubes | Numerical | $KNO_3$ | Stainless steel | Superheated vapour | Finned – plain tube | Percentage of improvement depending on number of fins and geometrical parameters | 2014 | Jung and Boo [7] |

*n.a*: not available

# 3. Combination of highly conductive materials with TES material

A very promising thermal conductivity enhancement technique, which has gained more relevance during the last years in the scientific community, is the combination of highly thermal conductive materials with the already known TES materials in order to obtain new composites with improved thermal properties. Within this group, three enhancement techniques have been studied: graphite composites, metal foams composites and the nanomaterials.

## 3.1 Graphite composites

Among the highly conductive materials used in combination with the TES material as heat transfer enhancers, graphite has been used not only because of its high thermal conductivity but also for its low density, its chemical resistance to corrosive environments and its suitability for high temperature processes [20]. Several natures of graphite can be combined with the TES material (Fig. 8) and four different routes can be perform to obtain a TES material-graphite composite [21]: by (1) impregnating or infiltrating (with/without vacuum) the TES material within the graphite matrix, by (2) mechanically dispersing or kneading graphite powders within the molten TES material, by (3) compressing at room temperature a previous mixture of the TES material and graphite powders and by (4) performing the electrospinning method in nano and micro scale.

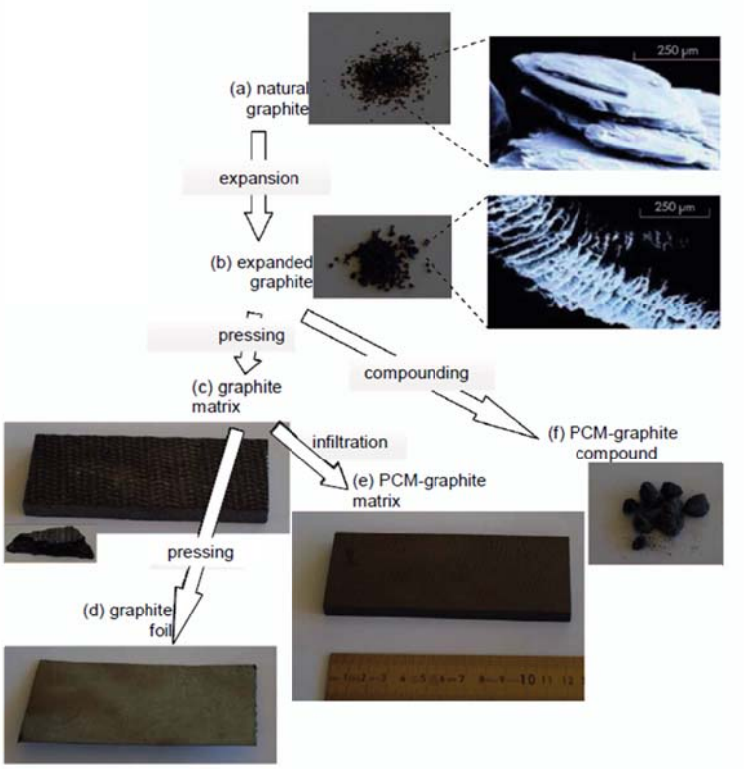


Fig. 8. Processing of graphite from the natural graphite to different products [20].

Impregnation, infiltration and compression are found to have higher enhancement performance than dispersion due to the fact that in these three processes graphite particles are always connected between them forming a highly thermal conductive and interconnected network while in the dispersion process graphite microstructures are formed but are not fully connected. Moreover, graphite particles parameters such as shape, concentration, distribution and orientation within the compound are extremely important to accurately calculate the average thermal conductivity of the graphite composite. However, average thermal conductivity is not the only criteria to determine the optimum composite preparation route. It has also to bear in mind economics and porosity, which are closely linked to the storage density. This last property is often not keep primordial during the obtaining process of the composite and can lead to a significantly reduction in the latent heat value if it is too low and to a reduction on the capillarity force and therefore leakage of liquid TES material if it is too high [20][22]. Several experimental and numerical investigations have been carried out studying the graphite as thermal conductivity enhancer and the ones available up to mid-2015 are explained below.

From the experimental point of view, the first attempt to study graphite composites at high temperature was carried out by Do Couto et al. [23], who tested the behavior of $KNO_3/NaNO_3$-expanded graphite (EG) and $KNO_3/LiNO_3$-EG composites obtained by two different elaboration routes: compression and infiltration. Results showed that compressed composites had an enhancement in a factor up to 10 and infiltrated composites presented a thermal conductivity enhancement lower than the previous route but accentuated in the direction parallel to its layered structure.

Bauer et al. [24] focused on the enhancement of $KNO_3/NaNO_3$ by studying the effect of adding natural graphite (NG) and compressed expanded graphite (CEG) with the infiltration route and adding commercial EG (CFG 500) with the compression route varying the graphite concentration and orientation. Results showed an enhancement of the thermal conductivity in the range from 3 to 30 times if compared to the single TES material. Moreover, it was observed that the thermal conductivity of the composites prepared by compression strongly depended on their graphite concentration (the higher the graphite concentration, the higher the conductivity), on the temperature (the higher the temperature, the lower the conductivity) and on the orientation and the thermal conductivity of the composites prepared by infiltration reached high conductivities with small graphite concentration.

Several studies, under the framework of the European project DISTOR, numerically and experimentally tested at both laboratory and industrial scales the behavior of graphite-

$NaNO_3/KNO_3$ composites for solar thermal power plants using direct solar steam generation [9][10][25][26]. Different types of graphite (NG, EG and ground EG) and three different elaboration routes (dispersion, infiltration and cold compression) were studied. Results showed an enhancement on the thermal conductivity in a factor between 10 and 31. The percentage of enhancement was found to be dependent on the graphite particle size, the working temperature and elaboration route, (Fig. 9). Regarding to this last parameter, important constrains were observed: infiltration was found to be inefficient, dispersion composites presented isotropic properties and thermal conductivity intensification and cold compressed composites presented highly anisotropic properties and strong intensification in thermal conductivity as well as important salt leakages.

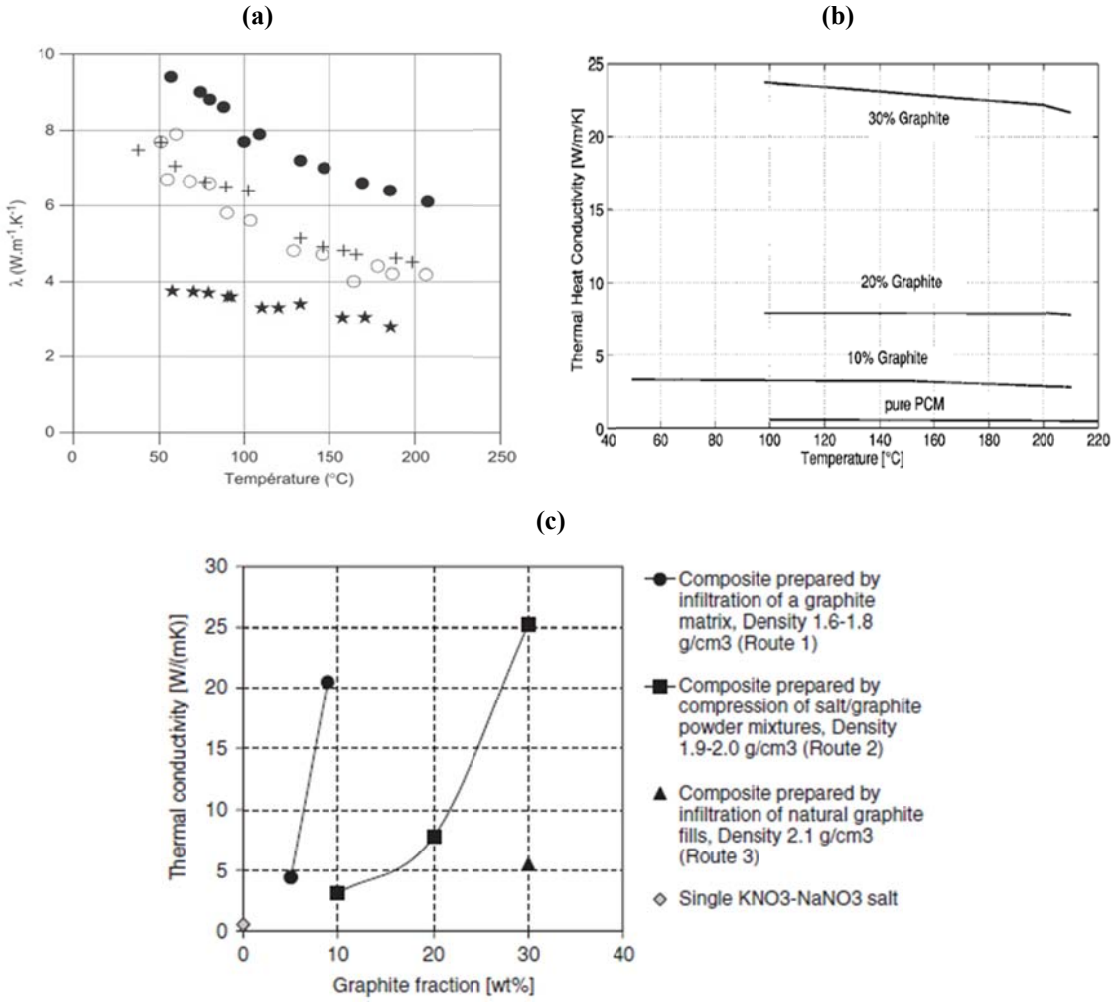


Fig. 9. Variation of the NaNO3/KNO3-graphite composites thermal conductivity: (a) Depending on the temperature and the graphite type: (★) Graphite flakes I, (+) Graphite flakes II, (○) Natural graphite, (●) Expanded graphite powder [26]; (b) Depending on the graphite percentage [9]; (b)) Depending on the graphite percentage and elaboration route at 200 ºC [10].

Acem et al. [27] and Lopez et al. [28] experimentally tested the behavior of expanded natural graphite (ENG)-$KNO_3/NaNO_3$ composite elaborated through the cold-compression process, with two different compression routes: uni-axial and isostatic (Fig. 10). Results showed on the one hand an enhancement of the thermal conductivity in a factor of 20 times for 15-20%wt of graphite and on the other hand an orthotropic thermal behavior of the composites obtained by uni-axial compression and an isotropic thermal behavior as well as over pressurization and salt leakages of the composites obtained by isostatic compression.

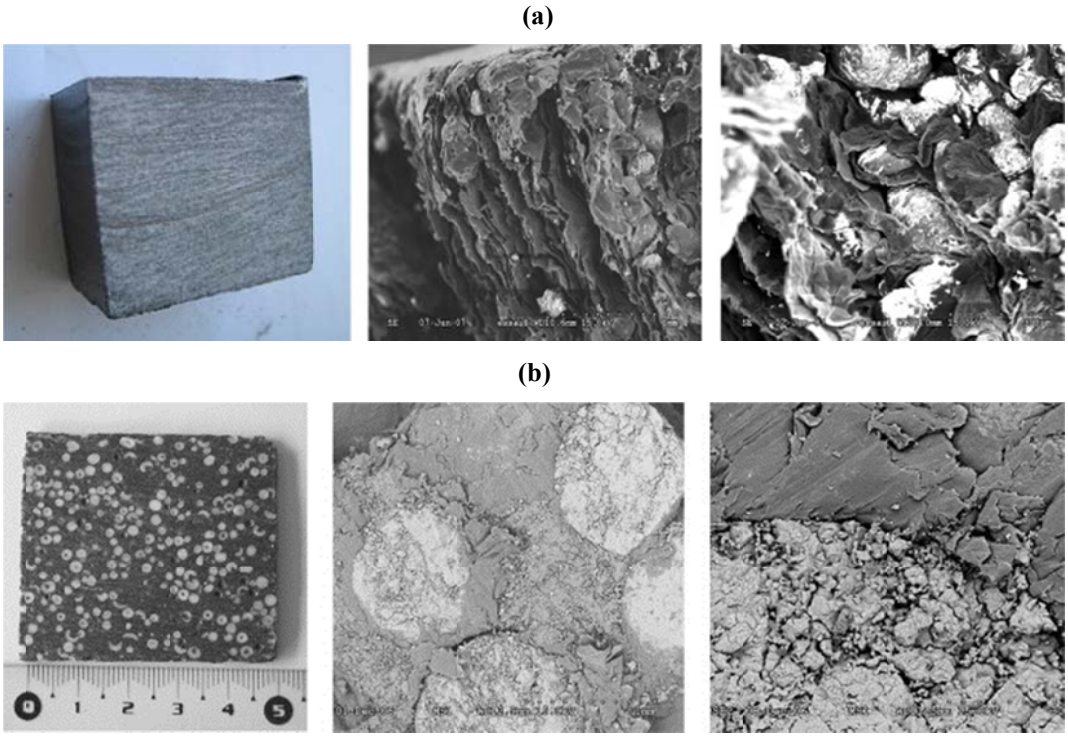


Fig. 10. (a) Graphite/salt composite obtained by uni-axial cold-compression route. Left: macroscopic scale. Center and right: microscopic scale. (b) Graphite/salt composite obtained by isostatic cold-compression route. Left: macroscopic scale. Center and right: microscopic scale [27].

Wu and Zhao [29] and Zhao and Wu [30] studied the feasibility of using EG-$NaNO_3$ composites elaborated through the dispersion route for high temperature applications. Results showed an enhancement of the heat transfer rate in both charging and discharging processes in a factor of 2.5, if compared to pure TES material because of the increasing in the thermal conductivity. However, this enhancement is reduced by half in the liquid region since the natural convection is hindered by the porous structures.

Yuan et al. [31] evaluated the behavior of cement-based TES materials-ground EG composites for sensible TES. Enhancements in a factor up to 2.96, depending on the cement heating treatment, were obtained.

Li and Zhang [32] studied the behavior of the $NaNO_3/LiNO_3$-EG composite elaborated through the dispersion route. Results showed a dependence of the thermal conductivity to the graphite concentration. Thermal conductivity enhancement values up to a factor of 10 could be achieved despite the fact that the effective latent heat was found to be reduced and the thermal stability was also found to have worse behavior.

Xiao et al. [33] studied the thermal performance of pure $NaNO_3$, $KNO_3$ and $KNO_3/NaNO_3$ as well as the composites made of such materials with various dispersed EG mass concentrations. Results showed an enhancement on the thermal conductivity in a 40 % depending on the EG mass concentration. Moreover, a variance on the melting/freezing temperatures of the composites was observed if compared with those of pure nitrates.

Huang et al. [34] studied the thermal behavior of EG- $LiNO_3$/KCl composites elaborated through the dispersion route. Results showed a thermal conductivity enhancement of the composites if compared with the eutectic $LiNO_3$/KCl in a factor range of 1.85–7.56, depending on the EG mass concentration and the apparent density of the composite, as well as a reduction on the heat storage period caused by the reduction of the phase change latent heat of the composite material.

Xiao et al. [35] reported a method to prepare $NaNO_3/KNO_3$-EG composites through the dispersion route with the addition of ultrasonic waves. Ultrasounds played the role of breaking EG into nanoscale slices and dispersing them into the nitrates. Results showed on one hand a good dispersion and a homogeneous distribution of the stripped graphite flakes within the composite and on the other hand no chemical reaction after the ultrasounds. Moreover, thermal conductivity enhancements in a factor of up to 2 and a latent heat reduction of 11% were observed.

Zhao et al. [36] studied the behavior of expanded natural graphite treated with sulfuric acid (ENG-TSA)-$KNO_3/NaNO_3$ composites in terms of anisotropic thermal conductivity, phase transition properties, thermal stability and micro structures. Results showed an enormous thermal conductivity enhancement, with values up to a factor of 110, a slight decrease in latent heat and no remarkable variation in the melting point. On the other hand, when the density of composite TES material and the salt mass fraction were high, problems with leakage of salt were found.

Zhong et al. [37] evaluated three different types of binary molten salts ($LiNO_3$/KCl, $LiNO_3$/$NaNO_3$ and $LiNO_3$/NaCl)-EG composites synthesized through the impregnation route. On one hand, results showed a thermal conductivity enhancement if compared to the pure eutectic mixture and on the other hand it was observed that these composites showed higher homogeneity and greater thermal stability (without loss of their morphologies and crystalline structures) in comparison to other salt-EG composites synthesized through infiltration or compression routes.

From the modelling and simulation point of view, Lafdi et al. [22] numerically studied and predicted the thermal performance of graphite foams infiltrated with TES materials for space TES applications. Results showed an improvement in a factor of 8 in the average value of the output power delivered to the working fluid as a result of the enhancement of the composite thermal conductivity.

Lopez et al. [28] studied the melting and solidification process in a $KNO_3$/$NaNO_3$-EG composite elaborated through the compression process. Results showed that during the melting process, the TES material volume expansion is constrained by the graphite creating an over pressurization that increases the melting point of TES material and decreases its latent heat. To avoid this problem, the authors identified the need to perform the following actions without reducing the effective thermal conductivity: reduce the pore-wall rigidity, increase the pore walls and/or increase the pores connectivity.

Kim et al. [38] and Zhao et al. [39] numerically studied the use of graphite foam-$MgCl_2$ composite in a LHTES system, consisting of a tank filled with a TES material and pipes carrying a heat transfer fluid simulating a CSP plant. Results showed that the thermal conductivity enhancement of the composite not only could improve the exergy efficiency in the system but also it could reduce the number of pipes of the system in a factor of 13.5 and therefore a huge reduction on the investment costs.

## 3.2 Metal foams composites

The concept of metal foam, also referred as cellular metals, porous metals, foamed metal and metallic foam [40], consists of a highly metallic porous material (solid metal containing a large volume fraction of gas pores) which is combined with TES materials. Two different types of foams can be differentiated depending on the pores characteristics: close-cell metallic foam if the pores are sealed or open-cell metallic foams if the pores form an interconnected network [41].

The concept of metal foams has been widely studied during the last decades in the automotive, aerospace, medical, environment, chemical, metallurgy, structural and mechanical engineering industries but it is currently starting to emerge as a promising thermal conductivity enhancement technique, not only because of its good intrinsic thermomechanical properties (mainly high thermal conductivity and good behavior at high temperature), but also because of the high versatility in the control of variables such as lightness, pore distribution, permeability, specific surface area to volume ratio and capillarity [42].

Focusing on metal foams as thermal conductivity enhancers, it has been found that very few studies have been carried out at high temperature. Chen et al. [41] reviewed the research progress of TES materials embedded with metal foams and studied the effects of introducing this enhancer on the conduction, convection and phase change heat transfer process of the composite. They observed on the one hand that metal foams composites have higher effective thermal conductivity and thus they could improve the uniformity of the temperature distribution but on the other hand, the presence of the metal foam reduce drastically the natural convection, for analogous reasoning than in the graphite composites, warning the researchers to consider the effects of porosity and pore size on both the conduction and convection heat transfer.

Wu and Zhao [29] and Zhao and Wu [30] experimentally tested the feasibility of using $NaNO_3$ embedded with copper and steel alloy metal foams (Fig. 11) (varying the porosity and pore density in cylindrical containers in order to enhance the heat transfer performance of the pure TES material. Results showed that the heat transfer rate could be enhanced by 2.5 times if compared to the pure $NaNO_3$ in the heating process from 250–300 °C. However, when this process took place in the liquid region, the heat transfer rate was reduced by half because of the suppression of the natural convection by the porous structures.

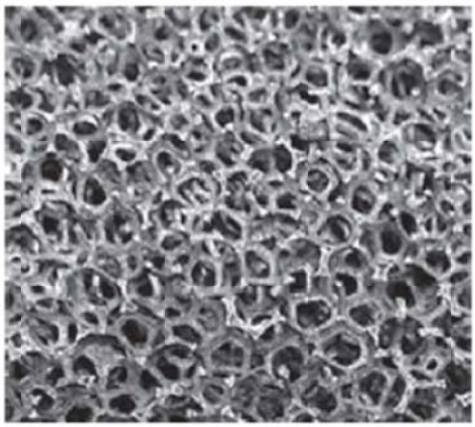

Fig. 11. Microscopical structure of a metal foam [29].

Zhang et al. [43] experimentally and numerically investigated the thermal enhancement of the eutectic mixture $KNO_3/NaNO_3$ by combining it with two different metal foams (copper and nickel foams). It was observed that during the charging process the presence of the metal foams weakened the influence of the natural convection and therefore limited the process. However, in the discharging process, where the conduction is the dominant mechanism, the presence of copper and nickel foams enhanced the process in 28.8% and 19.3% respectively.

Li and Wu [44] numerically investigated the thermal behavior of $NaNO_3$ inside porous copper matrix depending on porosity and pore density of the metal foam. Results showed a heat transfer coefficient enhancement in the solid state with values up to 28.1 times by heat conduction and an enhancement in the liquid state with values up to 3.1 times by the combination of natural convection and heat conduction. As a result, not only both the melting and the solidification processes are shortened but also the time differences between them were greatly shortened to harmonize the heating and cooling rates.

Yang et al. [45] [46] numerically studied the influence of varying the porosity and pore density in the enhancement of a copper metal foam composite. In the first study [45], a sandwich structure with fins and copper metal foam imbedded in $NaNO_3$ was used to evaluate the flow and heat transfer behavior. Results showed a significant improvement in the heat transfer performance. Moreover it was observed that when the porosity of the metal foam is decreased, the phase change period can be substantially shortened, while the effect of the pore density is not notable. In the second study [46], a $KNO_3$- copper metal foam composite was used. Results showed an improvement in the charging process performance up to 24.2 % by increasing linearly the porosity from the bottom to the top.

## 3.3 Nanomaterials

In the literature, the material composed by nanometer-sized particles (nanoparticles) and a base material (BM) is usually presented as nanofluid [47], when the BM is in the liquid state, or nanocomposite, when the BM is in the solid state [48]. However, in this review both concepts will be presented as nanomaterial to facilitate the understanding of the article.

The advance of technology has allowed the researchers to obtain smaller structures and take advantage of them in order to enhance the thermal properties of the actual TES materials. Previous studies have presented the advantages and disadvantages of nanomaterials if compared to pure materials [49][50][51][52][53][54][55]. Among the advantages, it can be found (1)

higher thermal capacity, which allows higher thermal storage in reduced spaces and therefore a reduction of cost, (2) higher effective thermal conductivity and higher specific surface, which enhance the heat transfer and decreases the charging and discharging processes, (3) a good stability on the dispersion of the nanoparticles within the TES material and reduced particle clogging, which allows the material not to have a variation on its properties, (4) liquid-like properties of the nanoparticles when the nanomaterial is melted, (5) reduction of the subcooling effect, since the nanoparticles can act as nucleating agents, and the most important, (6) the researcher can adjust the properties depending on the material of the nanoparticles, their concentration and distribution within the BM, their size and geometry and the interfacial effects between both the BM and the nanoparticles. On the other hand, some disadvantages have been observed in previous experiments, which are (1) the difficulty on their synthesis, (2) the difficulty on controlling the size and dimensions of the nanoparticles and (3) the toxicity of some of the nanomaterials for the humanity and/or environment.

Studies focused on the thermal conductivity enhancement with the dispersion of highly conductive particles are mainly based on water based fluids [50], which cover mid-low temperatures ranges. Very few studies covering thermal conductivity enhancements in the high temperature range have been performed since the research in this temperature range is mainly focused on the enhancement of specific heat.

Nanomaterials at high temperature are mainly obtained from two different synthesis methods [56]. The first method, known as two-step solution method or liquid solution method, was proposed by Shin and Banerjee [57] and is described as follows: first, both the nanoparticles and the BM are mixed, with their respectively fraction mass depending on the study case, in the dry state. Then, the dry mixture is dissolved in distilled water and the resulting mixture is homogeneously dispersed with ultrasounds. Finally, the homogenized mixture is dried on a hot plate. The second method, known as the stirring dispersion method, was proposed by Ho and Pan [58] and is described as follows: first, a crucible made of stainless steel is filled with the BM and the nanoparticles with their respectively fraction mass depending on the study case, in the dry state. Then, a stirrer made of stainless steel is placed inside the crucible and it is placed on a stirring hotplate were the dry mixture is melted and mixed. Finally, the mixture is cooled through forced convection by a cooling fan.

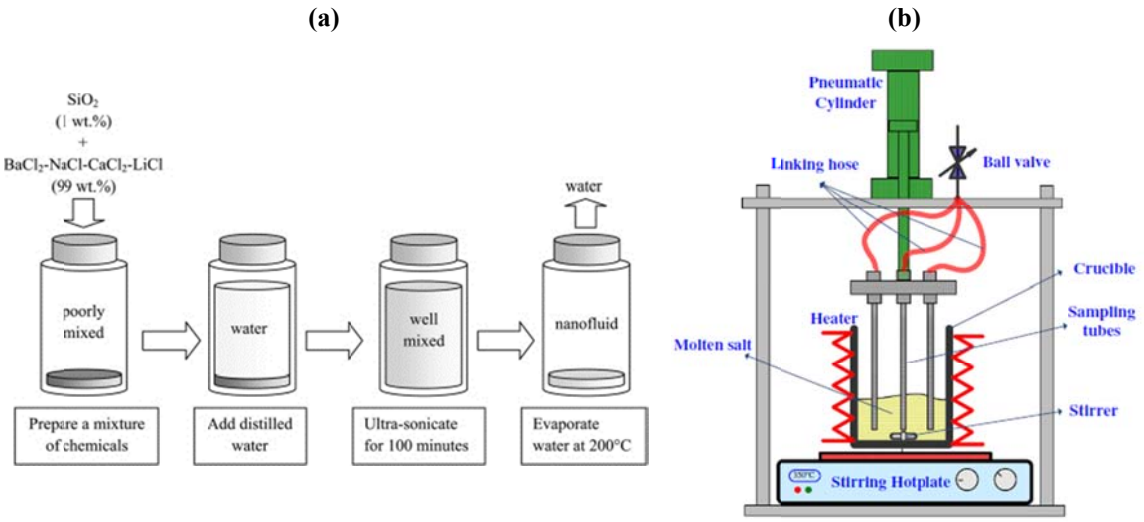


Fig. 12. (a) Schematic diagram of preparation of the two step solution method [57]. (b) Schematic diagram of preparation of the stirring dispersion method [58].

One of the first attempts to explain the capabilities of the addition of highly conductivity particles in order to enhance the effective thermal conductivity was Siegel [59], who numerically demonstrated an enhancement of 10-20 % on the heat transfer with 20 % volume of particles. More recently, some researchers [60][61][62][63] tried to explain the behavior of the nanoparticles within the TES material and the responsible phenomenon for thermal conductivity enhancement since the results obtained did not followed the classical theories. They stated that the possible phenomena responsible for the thermal conductivity enhancement of the nanomaterials were the clustering or aggregation of the nanoparticles, the Brownian motion of the nanoparticles, the nature of the heat transport in nanoparticles and/or the molecular layering of the BM at the interface with the nanoparticles [64].

Shi et al. [65] and Yuan et al. [66][67][68] studied the thermal properties of high temperature cementitious TES materials with the addition of $ZrO_2$, $SiO_2$, MgO and Cu nanoparticles. On the one hand, $ZrO_2$ nanoparticles [66] showed practically no enhancement if compared to the pure aluminate cement but on the other hand, $SiO_2$ [66], MgO [67] and Cu [68] nanoparticles showed noticeable enhancements with values up to 60 %.

Liu et al. [69] experimentally studied the characterization and the thermal performance of nanomaterials consisting on phase-change Bi nanoparticles embedded in an Ag matrix, by modifying the nanoparticle size, shape, and volume fraction in the composite. Results showed higher thermal conductivity enhancements if compared to the BM, when using smaller nanoparticle volume fractions and/or larger nanoparticles diameters.

Shin and Banerje [70] obtained a thermal conductivity enhancement of up to 45 % by dispersing 1% of $SiO_2$ nanoparticles in the eutectic mixture of $Li_2CO_3$ and $K_2CO_3$.

On the other hand, Ye et al. [71] and Tao et al. [72] studied the dispersion of different kinds of carbon nanostructures (single walled carbon nanotubes, SWCNT; multi-walled carbon nanotubes, MWCNT; graphene and fullerene C60) at different mass concentrations to different eutectic mixtures ($Na_2CO_3$/MgO and $Li_2CO_3$ /$K_2CO_3$). It was observed that the thermal conductivity could be increased up to 69 %.

Finally, Cingarapu et al. [73] and Timofeeva et al. [74] modified, instead of TES material as the previous studies did, the HTF Therminol 66 by adding core/shell Sn/$SiO_2$ (Fig. 13) and $SiO_2$ nanoparticles in it, respectively, observing enhancements of 17 % in the thermal conductivity of the modified HTF.

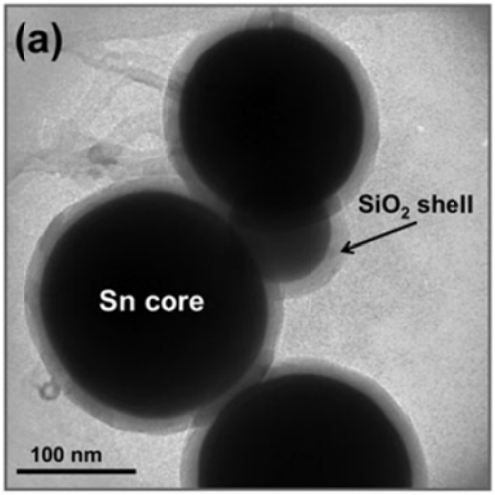


Fig. 13. Transmission electron microscopy images of Sm/$SiO_2$ nanoparticles [73].

Table 3, Table 4 and Table 5 review, in a chronological order, the different studies carried out concerning the enhancement technique of combining highly conductive materials with TES materials at high temperature, by showing the study case, the TES material improved, the enhancement material used (weight concentration and size) the synthesis method, the comparison performed, the improvement observed and the measurement instrument.

Table 3. Review of the studies concerning the combination of highly conductive material with TES material at high temperature. Case 3: Graphite composites.

| Study case | | Graphite type[1] (nominal size) | Concentration (wt%) | TES material | Method of synthesis | Comparison | Improvement and measurement instrument[2] | Year | Reference |
|---|---|---|---|---|---|---|---|---|---|
| 1 | Experimental | EG (n.a) | 15 | $KNO_3 + NaNO_3$ (54 + 46 wt%) $KNO_3 + LiNO_3$ (68 + 32 wt%) | Compression Infiltration | Different graphite composites (different routes) vs. pure TES materials | Up to a factor of 10 (15 wt%, compression, $KNO_3$-$NaNO_3$) Up to a factor higher than 10 (15 wt%, compression, $LiNO_3$-$NaNO_3$) By: TCCT | 2005 | Do Couto et al. [23] |
| 2 | Experimental | NG (n.a) CEG (n.a) CFG 500 (n.a) | 5/10/20/30 | $KNO_3 + NaNO_3$ (n.a. wt%) | Compression Infiltration | Different graphite composites (different routes, graphite types and concentrations) vs. pure TES materials | Up to a factor of 30 (30 wt%, compression) By: LFA457 (Netzsch Gertebau) | 2006 | Bauer et al. [24] |
| 3 | Numerical | Graphite foam (n.a.) | n.a. | $LiF–CaF_2$ (n.a. %) | n.a. | Graphite composites vs pure TES material | *Output power delivered:* Up to 800 % | 2008 | Lafdi et al. [22] |
| 4 | Experimental | NG (400 µm) EG (n.a.) GEG (50-500 µm) | 7/10/20/30 | $KNO_3$-$NaNO_3$ (n.a. %) | Dispersion Infiltration Cold compression | Different graphite composites (different routes, graphite types and | Up to a factor of 31 (20 wt%, compression) Up to a factor of 10 (7 wt%, dispersion) | 2008 | Pincemin et al. [25] |

| | | | | | | | | | |
|---|---|---|---|---|---|---|---|---|---|
| | | | | | | concentrations) vs. pure TES materials | By: n.a. | | |
| 5 | Experimental Numerical | NG (6/15/44/75/150/ 400 µm) EG (n.a.) GEG (50-500 µm) | 10/20/30 | $KNO_3$ + $NaNO_3$ (50 + 50 mol%) $ZnCl_2$ + KCl (31.9 + 68.1 mol%) $NaNO_3$ $KNO_3$ NaOH KOH $ZnCl_2$ | Impregnation Dispersion | Different graphite composites (different routes, graphite types and concentrations) vs. pure TES materials | Up to a factor of 10 (20 wt%, CEG, 6 µm, dispersion) By: n.a. | 2008 | Pincemin et al. [26] |
| 6 - 7 | Theoretical | NG (n.a.) EG (0.5-1.0 mm) | 10/20/30 | $KNO_3$ + $NaNO_3$ (n.a. %) | Compression Infiltration | Different graphite composites (different routes, graphite types and concentrations) vs. pure TES materials | Up to a factor of 20 (30 wt%, compression) By: n.a. | 2008 | Steinmann and Tamme [9] Tamme et al. [10] |
| 8 | Experimental | ENG (500 µm) | 4.75/5/5.93/7.11 /8.29/9.46/10/15 /20/25/30 | $KNO_3$ + $NaNO_3$ (50 + 50 mol%) | Compression uni-axial Compression isostatic | Different graphite composites (different routes and graphite concentrations) vs. pure TES materials | Up to a factor of 20 (20 wt%, compression) By: THP method | 2010 | Acem et al. [27] |

| | | | | | | | | | |
|---|---|---|---|---|---|---|---|---|---|
| 9 | Numerical | ENG (500 µm) | 5/10/15 | $KNO_3$ + $NaNO_3$ (50 + 50 mol%) | Compression uni-axial Compression isostatic | Different graphite composites (different routes and graphite concentrations) vs. pure TES materials | *Investment costs:* Up to 45 % (10 wt%, compression) | 2010 | Lopez et al. [28] |
| 10 - 11 | Experimental | EG | 3/6 | $NaNO_3$ | Dispersion | Graphite composite vs pure TES material | *Heat transfer rate*: 190 % | 2011 | Wu and Zhao [29] Zhao and Wu [30] |
| 12 | Experimental | GEG (n.a.) | 1/5/10/15 | Aluminate cement | Dispersion | Graphite composites vs pure TES material | Up to a factor of 1.89 (15wt%, dispersion) By: TCCT (TPS2500, Hot Disk Ltd.) with Probe 5465 | 2012 | Yuan et al. [31] |
| 13 | Experimental | EG (n.a.) | 10/20/30 | $NaNO_3$ + $LiNO_3$ (45 + 55 mol%) | Dispersion | Graphite composites vs pure TES material | Up to a factor of 10 (30wt%, dispersion) By: TCCT (TPS2500, Hot Disk Ltd.) with Probe 5465 | 2013 | Li and Zhang [32] |
| 14 | Experimental | EG (n.a.) | 5/10 | $KNO_3$ + $NaNO_3$ (different wt%) | Dispersion | Graphite composites vs pure TES material | Up to 40 % (10 wt%, dispersion) By: THM | 2013 | Xiao et al. [33] |
| 15 | Numerical | Graphite foam | n.a. | $MgCl_2$ | n.a. | Graphite composite | *Number of pipes*: | 2014 | Kim et al. |

| | | | | | | | | | |
|---|---|---|---|---|---|---|---|---|---|
| | | | | | | vs pure TES material | Reduction in a factor of 13.6 | | [38] |
| 16 | Experimental | EG (n.a) | 10/15/20/25/30 | $LiNO_3$ + KCl (n.a. %) | Dispersion | Graphite composites vs pure TES material | Up to a factor of 7.56 (30wt%, dispersion) By: TCCT (TPS2500, Hot Disk Ltd.) with Probe 5465 | 2014 | Huang et al. [34] |
| 17 | Experimental | EG (150 μm) | 0.5/1/1.5/2 | $KNO_3$ + $NaNO_3$ (60 + 40 mol%) | Dispersion | Graphite composites vs pure TES material | Up to a factor of 2.15 (2wt%, dispersion) By: LFA457 (Netzsch Gertebau) | 2014 | Xiao et al. [35] |
| 18 | Experimental | ENG treated with sulfuric acid (n.a) | 10/15 | $KNO_3$ + $NaNO_3$ (n.a. %) | Cold compression | Graphite composites vs pure TES material | Up to a factor of 100 (15wt%, compression) By: LFA457 (Netzsch Gertebau) | 2014 | Zhao et al. [36] |
| 19 | Numerical | Graphite foam (n.a.) | n.a. | $MgCl_2$ | n.a. | Graphite composite vs pure TES material | *Number of pipes*: Reduction in a factor of 13.6 *Exergy efficiency*: Up to 71 % | 2014 | Zhao et al. [39] |
| 20 | Experimental | EG (200-500 μm) | 10/12.5 | $LiNO_3$ + KCl (58.1 + 41.9 mol%) $LiNO_3$ + $NaNO_3$ | Impregnation | Different graphite composites (different graphite concentrations) vs. | Up to a factor of 7.87 (12.5wt%, impregnation) B By: TCCT (TPS2500, Hot Disk Ltd.) with | 2014 | Zhong et al. [37] |

| | | | | | | | | | |
|---|---|---|---|---|---|---|---|---|---|
| | | | | (49 + 51 mol%) $LiNO_3$ + NaCl (87 + 13 mol%) | | pure TES materials | Probe 5465 | | |

[1] *EG*: Expanded graphite / *NG*: Natural graphite / *CEG*: Compressed expanded graphite / *CFG*: Commercial expanded graphite / *GEG*: Ground expanded graphite / *ENG*: Expanded natural graphite / *MWCNT*: Multi-walled carbon nanotubes

[2] *SSCM:* Steady state comparative method / *THP*: Transient hot plate / *LFA*: Laser Flash Analysis / *TCCT*: thermal conductivity constant tester / *THW:* Transient hot wire

*n.a.:* not available

Table 4. Review of the studies concerning the combination of highly conductive material with TES material at high temperature. Case 4: Metal foams composites.

| Study case | | Porous material | Pore density (PPI[1]) | Porosity (ε) | TES material (mol%) | Comparison | Improvement | Year | Reference |
|---|---|---|---|---|---|---|---|---|---|
| 1 – 2 | Experimental | Copper<br>Copper - Steel alloy | 10/20/30 | 90/95 % | $NaNO_3$ | Different metal foam composites (PPI and porosity) vs pure TES material | *Heat transfer rate*:<br>Heating process up to 210 % | 2011 | Wu and Zhao [29]<br>Zhao and Wu [30] |
| 3 | Numerical | Copper | 5/10/20/30 | 90/95 % | $NaNO_3$ | Metal foam composite (porosity and pore density) vs pure TES material | *Melting process time:*<br>Up to a factor of 4.86 (ε=0.90, 10 PPI)<br>*Solidification process time:*<br>Up to a factor of 28.38 (ε=0.90, 30 PPI) | 2013 | Li and Zhang [32] |
| 4 | Numerical | Copper | 20/30/40 | 90 % | $NaNO_3$ | Effect of pore density and porosity | No numerical comparison was made with pure TES material | 2013 | Yang et al. [45] |
| 5 | Numerical | Copper | 20/30/40 | 88/90/92 % | $NaNO_3$ | Metal foam composite (porosity and pore density) vs pure TES material | *Melting process time:*<br>Up to 17.94 % (ε=0.92, 40 PPI)<br>*Solidification process time:*<br>Up to 4.28 % (ε=0.90, 30 PPI) | 2015 | Yang et al. [46] |

| | | | | | | | | | |
|---|---|---|---|---|---|---|---|---|---|
| 6 | Experimental<br>Numerical | Copper<br>Nickel | 10 | 96.5/97.5 % | $KNO_3$ + $NaNO_3$<br>(50 + 50 %) | Different metal foam composites (material) vs pure TES material | *Solidification process time (Copper):*<br>Up to 28.8 % (ε=0.96, 10 PPI)<br>*Solidification process time (Nickel):*<br>Up to 19.3 % (ε=0.97, 10 PPI) | 2015 | Zhang et al. [43] |

[1] *PPI*: Pore number per inch

Table 5. Review of the studies concerning the combination of highly conductive material with TES material at high temperature. Case 5: Nanomaterials.

| Study case | | Nanoparticles (nominal size) | Concentration (wt%) | TES material (mol%) | Method of synthesis | Comparison | Improvement and measurement instrument[1] | Year | Reference |
|---|---|---|---|---|---|---|---|---|---|
| 1 | Numerical | n.a. | 20/60 | Molten salts | n.a. | Concentration of nanoparticles | *Heat transfer rate*: Solidification process up to 20 % | 1977 | Siegel [59] |
| 2 | Experimental | $SiO_2$ (15 nm) | 1.2/3.6/5.0/7.0 | Therminol 66 | Two-step solution method | Concentration of nanoparticles | Up to 17.1 % (7.0 wt%, at 25 ºC) By: THW (Model KD2pro, Decagon Devices, Inc.) | 2011 | Timofeeva et al. [74] |
| 3 | Experimental | $ZrO_2$ (20 nm) | 1.0/2.0/3.0/4.0/5.0 | Aluminate cement | Normal mixture | Concentration of nanoparticles | Practically no enhancement By: TCCT (TPS2500, Hot Disk Ltd.) with Probe 5465 | 2013 | Yuan et al. [66] |
| 4 | Experimental | $Sn/SiO_2$ (50-100 nm) | 1.0/2.0/3.0/4.0/5.0 | Therminol 66 | Two-step solution method | Concentration of nanoparticles | Up to 17.1 % (5.0 wt%) By: THW (Model KD2pro, Decagon Devices, Inc.) | 2014 | Cingarapu et al. [73] |
| 5 | Experimental | $SiO_2$ (50 nm) | 1.0/2.0/3.0/4.0/5.0 | Aluminate cement | Similar to stirring method | Concentration of nanoparticles | Up to 61 % (3.0 wt%) By: TCCT (TPS2500, Hot Disk Ltd.) with Probe 5465 | 2014 | Shi et al. [65] |
| 6 | Experimental | MWCNT (11 nm x 10 μm) | 0.1/0.2/0.3/0.5 | $Na_2CO_3$ + MgO (40 + 60 %, 50 + 50 %, 60 + 40 %, 80 + 20 %) | Normal mixture | Concentration of nanoparticles | Up to 69 % (0.5 wt%) By: UNITHERM™ model 2022 (Anter Corporation) | 2014 | Ye et al. [71] |
| 7 | Experimental | MgO (50 nm) | 2.0/3.0/4.0/10.0 | Aluminate cement | Normal mixture | Concentration of nanoparticles and | Up to 35.4 % (1 wt%, 350 ºC) | 2014 | Yuan et al. [67] |

| | | | | | | | | | |
|---|---|---|---|---|---|---|---|---|---|
| | | | | | | temperature effect | Up to 23.6 % (1 wt%, 350 ºC)<br>By: TCCT (TPS2500, Hot Disk Ltd.) with Probe 5465 | | |
| 8 | Experimental | Bi (8.1/9.8/13.2/14.9 nm) | 2.0/5.0/10.0 | Ag | Normal mixture | Concentration of nanoparticles and nanoparticle size | Decrease if concentration increases<br>By: n.a. | 2015 | Liu et al. [69] |
| 9 | Experimental | $SiO_2$ (10-30 nm) | 1.0 | $Li_2CO_3 + K_2CO_3$ (62 + 38 %) | Two-step solution method | Nanomaterial vs pure material | Up to 47 % (1 wt%, 150 ºC)<br>Up to 36 % (1 wt%, 250 ºC)<br>Up to 37 % (1 wt%, 350 ºC)<br>By: LFA 447 Nanoflash (Netzsch Instruments N.A. LLC.). | 2015 | Shin and Banerjee [70] |
| 10 | Experimental | SWCNT (5-20 nm x 1-5 µm)<br>MWCNT (10-50 nm x 0.5-1 µm)<br>Graphene (10-20 nm x 1-5 µm)<br>Fullerene $C_{60}$ (0.5-2 µm) | 0.1/0.5/1.0/1.5/2.5 | $Li_2CO_3 + K_2CO_3$ (62 + 38 mol%) | Two-step solution method | Type of nanoparticles and concentration of nanoparticles | *SWCNT:* Up to 56.98 % (1.5 wt%)<br>*MWCNT:* Up to 50.05 % (1.5 wt%).<br>*Graphene*: Up to 27.77 % (2.5 wt%)<br>$C_{60}$*:* Up to -31.85 % (2.5 wt%)<br>By: LFA | 2015 | Tao et al. [72] |
| 11 | Experimental | Cu powder | 1.0/5.0/10.0/15.0 | Aluminate cement | Normal mixture | Concentration of nanoparticles and temperature | Up to 24 % (15 wt%, 105 ºC)<br>Up to 50 % (15 wt%, 350 | 2015 | Yuan et al. [68] |

| | | | | | | | | | |
|---|---|---|---|---|---|---|---|---|---|
| | | | | | | effect | ºC)<br>Up to 51 % (15 wt%, 900 ºC)<br>By: TCCT (TPS2500, Hot Disk Ltd.) with Probe 5465 | | |

[1] *EG*: Expanded graphite / *NG*: Natural graphite / *CEG*: Compressed expanded graphite / *CFG*: Commercial expanded graphite / *GEG*: Ground expanded graphite / *ENG*: Expanded natural graphite / *MWCNT*: Multi-walled carbon nanotubes / *SWCNT*: Single -walled carbon nanotubes

[2] *THW:* Transient hot wire / *TCCT*: thermal conductivity constant tester / *LFA*: Laser Flash Analysis

*n.a.:* not available

# 4. Overview of the enhancement techniques research evolution

The Technology Readiness Level (TRL) of the five enhancement techniques reviewed in the present study are presented as well as the temporal evolution of the publications related to them. The main objective of this classification is to give an overview about how the maturity of the enhancement techniques is in order to describe recent trends in this field and to identify a niche of research.

TRL is a measurement system used on the one hand to assess the maturity of evolving technologies during their development and early operations and on the other hand to compare technologies [75]. This scale classifies the maturity of a technology in nine levels, from the basic research until its commercial application (Table 6).

Table 6. Technology readiness levels summary. Based on: [76][77].

| Level | Definition |
|---|---|
| TRL 1 | Basic principles observed |
| TRL 2 | Technology concept formulated |
| TRL 3 | Experimental proof of concept at lab scale |
| TRL 4 | Technology validated in small-scale |
| TRL 5 | Development at real-scale |
| TRL 6 | System prototype demonstration in simulated operational environment |
| TRL 7 | System prototype demonstration in real operational environment |
| TRL 8 | System complete and qualified, first commercial prototype |
| TRL 9 | Commercial application |

As it can be observed in Table 7, the 40.4 % and the 53.8 % of the studies reviewed are in a TRL 2 and TRL 3, respectively, which means that more than the 94 % of the work carried out so far is still in the very early stages. The promising aspects of each thermal enhancement techniques have been detected and observed. Moreover, active research and development has gained relevance and the governments have been started to fund projects related with numerical and laboratory scale experimentation in order to validate the analytical predictions. Only the 6 % of the experimentation has been carried out at a scale higher than the laboratory. Therefore, since the benefits of implementing the thermal conductivity enhancement techniques have been already proved, the next step is to test them at higher scale in order to validate the results obtained numerically and at laboratory scale.

Moreover, the tendency of the research groups in terms of implementing and evaluating the different thermal enhancement techniques reviewed in the present study have been also studied in order to show the evolution of their investigation in the last 10 years (Fig. 14). It can be seen that during the first years of this period, only the implementation of extended surfaces was studied, since it is a technique that was previously demonstrated at lower temperatures. However, as both the composites technology and nanotechnology have gained relevance and observing the promising results at lower temperatures, researchers are focusing their thermal enhancement work at studying them.

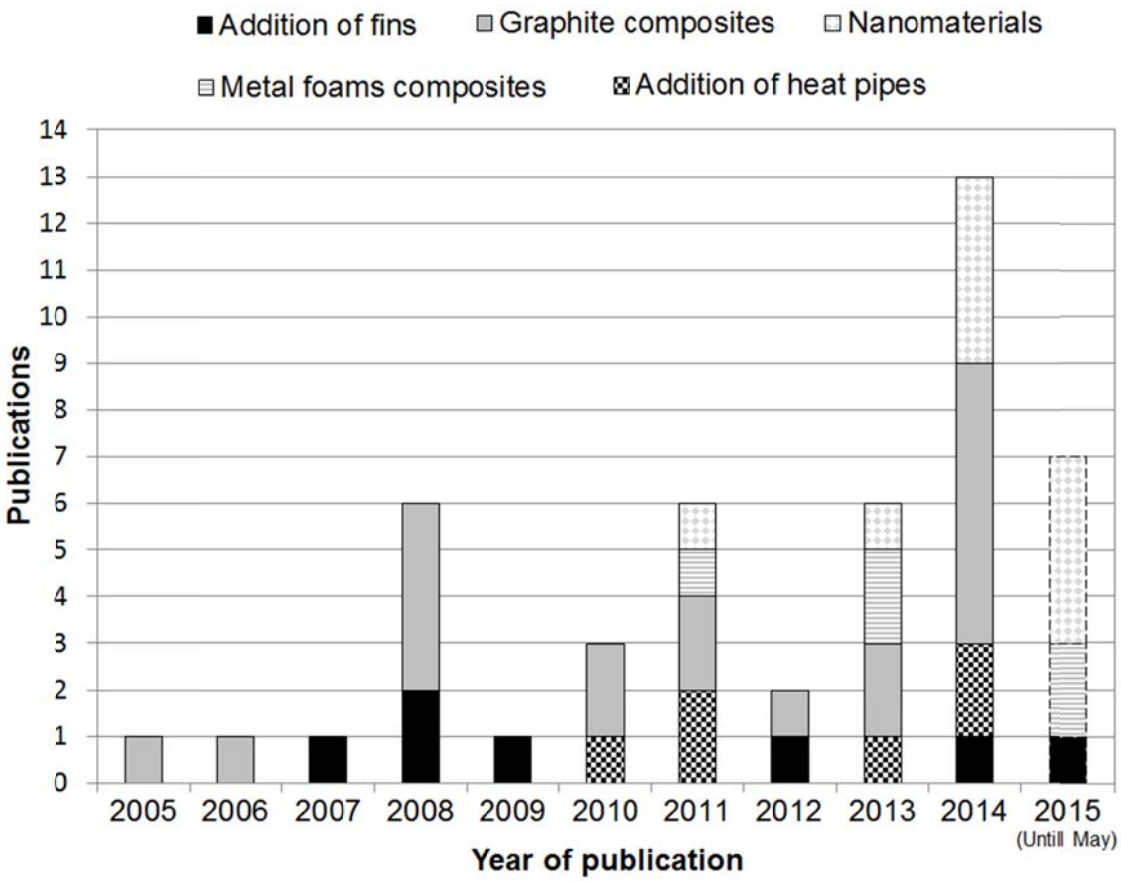


Fig. 14. Evolution of publication related with the thermal conductivity enhancement techniques at the high temperature field for the period 2005-mid 2015.

Table 7. Technology readiness levels (TRLs) of the different research work carried out in terms of thermal conductivity and specific heat enhancement techniques at high temperature at 2015.

| | | | TRL 1 | TRL 2 | TRL 3 | TRL 4 | TRL 5 | TRL 6-9 |
|---|---|---|---|---|---|---|---|---|
| **Enhancement technique** | **Addition of extended surfaces** | **Addition of fins** | - | [3] [4] [5] [6] [8] [12] | - | [10][13] | [11] | - |
| | | **Addition of heat pipes** | - | [7] [14] [16] [17] [18] [19] | - | - | - | - |
| | **Combination of highly conductive materials with TES material** | **Graphite composites** | - | [9] [10] [22] [38] [36] | [23] [24] [25] [26] [27] [28] [29] [30] [31] [32] [33] [34] [35] [39] [37] | - | - | - |
| | | **Metal foams composites** | - | [32] [45] [46] | [29] [30] [43] | - | - | - |
| | | **Nanomaterials** | - | [59] | [65] [66] [67] [68] [69] [70] [71] [72] [73] [74] | - | - | - |

## 5. Conclusions

One of the main obstacles that hinder the fully development and implementation of TES systems is the low thermal conductivity values that most of the currently commercial TES materials have. The present paper presents an exhaustive review of the numerical and experimental studies, involving the different thermal conductivity enhancement techniques, developed at the high temperature field (> 150 ºC). Notice that Part 1 of this article identifies and reviews more than 25 different requirements that TES materials and systems should consider for being used at those temperatures and the approaches to achieve them. The research is focused on the literature available on scientific journals until mid-2015 and the authors would like to apology if any paper has been neglected since the present paper does not claim about its exhaustiveness in the high temperature field.

The main conclusion regarding the different enhancement techniques are:

- **Extended surfaces**

  The addition of extended surfaces is the most and widely studied thermal conductivity enhancement techniques in the low temperature range (<150 ºC). Therefore, since its enhancement has been demonstrated, only little research has been carried out at high temperature.

  - *Addition of fins*

    It has been numerically and experimentally demonstrated the thermal performance improvement of this technique. Among all materials tested at high temperature, aluminum is preferred as fin material and the geometry of the fin is a key factor on the percentage of improvement. However, two main drawbacks have been observed, which are the increase of costs and the decrease of the packing factor.

  - *Addition of heat pipes*

    This technique has been only numerically studied at high temperature. Different parameters have been simulated and evaluated and in all the research work carried out, promising results were obtained.

- **Combination of highly conductive materials with TES material**

  The combination of highly thermal conductive materials with the already known TES materials in order to obtain new materials with improved thermal properties is gaining relevance every year.

  - *Graphite composites*

    Graphite is considered a good thermal conductivity enhancer not only because of its high thermal conductivity but also for its low density, its chemical resistance to

corrosive environments and its suitability for high temperature processes. Among the different graphite composites elaboration routes, impregnation and compression are found to have a high enhancement performance. Experimental results showed that the effective thermal conductivity of the composite strongly depends on the graphite fraction of the composite, the temperature and on the graphite particles size and orientation. However, a reduction on the natural convection has been observed in the liquid state.

- *Metal foams composites*

  Metal foams are promising thermal conductivity enhancers not only because of its good intrinsic thermomechanical properties, but also because of variables such as lightness, pore distribution, permeability, specific surface area to volume ratio and capillarity that can be controlled by the researchers. Very little experimentation has been carried at high temperature but results showed an increase of the thermal conductivity on the solid state and solidification process but no increase of the thermal conductivity on the liquid state and melting process due to the fact that the presence of metal foam reduce drastically the natural convection

- *Nanomaterials*

  The dispersion of nanoparticles within a TES material is the most promising enhancement technique for its implementation at industrial scale due to their advantages such as high thermal capacity, high effective thermal conductivity and specific surface, good stability on the dispersion of the nanoparticles within the TES material and reduced particle clogging, reduction of the subcooling effect and the most important, the researcher can adjust the properties depending on the material of the nanoparticles. Therefore, all the work done is focused on improving the most common TES materials used in solar plants. Results showed good and promising enhancement in thermal conductivity values.

Finally, the authors would like the readers to be critical with the results collected in the present review, since the lack of international standards or agreements in the expert community for evaluating the thermal properties of TES materials makes difficult to properly discuss and compare the results.

## Acknowledgments

The work is partially funded by the Spanish government (ENE2011-22722 and ULLE10-4E-1305). The authors would like to thank the Catalan Government for the quality accreditation

given to their research group GREA (2014 SGR 123). The research leading to these results has received funding from the European Union's Seventh Framework Programme (FP7/2007-2013) under grant agreement n° PIRSES-GA-2013-610692 (INNOSTORAGE). Laia Miró would like to thank the Spanish Government for her research fellowship (BES-2012-051861).

## References


[1] Gasia J, Miró L, Cabeza LF. Materials and system requirements of high temperature thermal energy storage systems: A review. Part 1: General requirements 2015; in press.

[2] Jegadheeswaran S, Pohekar SD. Performance enhancement in latent heat thermal storage system: A review. Renew Sustain Energy Rev 2009;13:2225–44. doi:10.1016/j.rser.2009.06.024.

[3] Zhang Y, Faghri A. Heat transfer enhancement in latent heat thermal energy storage system by using the internally finned tube. Int J Heat Mass Transf 1996;39:3165–73. doi:10.1016/0017-9310(95)00402-5.

[4] Seeniraj RV, Velraj R, Narasimhan NL. Thermal analysis of a finned-tube LHTS module for a solar dynamic power system. Heat Mass Transf 2002;38:409–17. doi:10.1007/s002310100268.

[5] Khaled A-RA. Heat transfer enhancement in hairy fin systems. Appl Therm Eng 2007;27:250–7. doi:10.1016/j.applthermaleng.2006.04.012.

[6] Guo C, Zhang W. Numerical simulation and parametric study on new type of high temperature latent heat thermal energy storage system. Energy Convers Manag 2008;49:919–27. doi:10.1016/j.enconman.2007.10.025.

[7] Jung EG, Boo JH. Thermal analytical model of latent thermal storage with heat pipe heat exchanger for concentrated solar power. Sol Energy 2014;102:318–32. doi:10.1016/j.solener.2013.11.008.

[8] Tiari S, Qiu S, Mahdavi M. Numerical study of finned heat pipe-assisted thermal energy storage system with high temperature phase change material. Energy Convers Manag 2015;89:833–42. doi:10.1016/j.enconman.2014.10.053.

[9] Steinmann W-D, Tamme R. Latent Heat Storage for Solar Steam Systems. J Sol Energy Eng 2008;130:5. doi:10.1115/1.2804624.

[10] Tamme R, Bauer T, Buschle J, Laing D, Muller-Steinhagen H, Steinmann W-D. Latent heat storage above 120°C for applications in the industrial process heat sector and solar power generation. Int J Energy Res 2008;32:264–71. doi:0.1002/er.1346.

[11] Laing D, Bauer T, Steinmann W-D, Lehmann D. Advanced high temperature latent heat storage system – design and test results. 11th Int. Conf. Therm. Energy Storage, Stockholm: 2009.

[12] Tao YB, He YL, Qu ZG. Numerical study on performance of molten salt phase change thermal energy storage system with enhanced tubes. Sol Energy 2012;86:1155–63. doi:10.1016/j.solener.2012.01.004.

[13] Gil A, Oró E, Miró L, Peiró G, Ruiz Á, Salmerón JM, et al. Experimental analysis of hydroquinone used as phase change material (PCM) to be applied in solar cooling refrigeration. Int J Refrig 2014;39:95–103. doi:10.1016/j.ijrefrig.2013.05.013.

[14] Shabgard H, Bergman TL, Sharifi N, Faghri A. High temperature latent heat thermal energy storage using heat pipes. Int J Heat Mass Transf 2010;53:2979–88. doi:10.1016/j.ijheatmasstransfer.2010.03.035.

[15] Siddique M, Khaled A-RA, Abdulhafiz NI, Boukhary AY. Recent Advances in Heat Transfer Enhancements: A Review Report. Int J Chem Eng 2010;2010:1–29. doi:10.1155/2010/106461.

[16] Nithyanandam K, Pitchumani R. Analysis and optimization of a latent thermal energy storage system with embedded heat pipes. Int J Heat Mass Transf 2011;54:4596–610. doi:10.1016/j.ijheatmasstransfer.2011.06.018.

[17] Nithyanandam K, Pitchumani R. Thermal energy storage with heat transfer augmentation using thermosyphons. Int J Heat Mass Transf 2013;67:281–94. doi:10.1016/j.ijheatmasstransfer.2013.08.007.

[18] Khalifa A, Tan L, Date A, Akbarzadeh A. A numerical and experimental study of solidification around axially finned heat pipes for high temperature latent heat thermal energy storage units. Appl Therm Eng 2014;70:609–19. doi:10.1016/j.applthermaleng.2014.05.080.

[19] Robak CW, Bergman TL, Faghri A. Economic evaluation of latent heat thermal energy storage using embedded thermosyphons for concentrating solar power applications. Sol Energy 2011;85:2461–73. doi:10.1016/j.solener.2011.07.006.
[20] Mehling H, Cabeza LF. Heat and cold storage with PCM. Berlin, Heidelberg: Springer Berlin Heidelberg; 2008.
[21] Nomura T, Okinaka N, Akiyama T. Technology of Latent Heat Storage for High Temperature Application: A Review. ISIJ Int 2010;50:1229–39. doi:10.2355/isijinternational.50.1229.
[22] Lafdi K, Mesalhy O, Elgafy A. Graphite foams infiltrated with phase change materials as alternative materials for space and terrestrial thermal energy storage applications. Carbon 2008;46:159–68. doi:10.1016/j.carbon.2007.11.003.
[23] Do Couto K., Tamme R, Müller-Steinhagen H. PCM-Graphite storage materials for the temperature range 100-300°C, Yverdon-Les-Bains, Schweiz: 2005.
[24] Bauer T, Tamme R, Christ M, Öttinger O. PCM-Graphite Composites for High Temperature Thermal Energy Storage. Tenth Int. Conf. Therm. Energy Storage, Pomona, NJ (USA): 2006.
[25] Pincemin S, Py X, Olives R, Christ M, Oettinger O. Elaboration of Conductive Thermal Storage Composites Made of Phase Change Materials and Graphite for Solar Plant. J Sol Energy Eng 2007;130:011005–011005. doi:10.1115/1.2804620.
[26] Pincemin S, Olives R, Py X, Christ M. Highly conductive composites made of phase change materials and graphite for thermal storage. Sol Energy Mater Sol Cells 2008;92:603–13. doi:10.1016/j.solmat.2007.11.010.
[27] Acem Z, Lopez J, Palomo Del Barrio E. KNO3/NaNO3 – Graphite materials for thermal energy storage at high temperature: Part I. – Elaboration methods and thermal properties. Appl Therm Eng 2010;30:1580–5. doi:10.1016/j.applthermaleng.2010.03.013.
[28] Lopez J, Caceres G, Palomo Del Barrio E, Jomaa W. Confined melting in deformable porous media: A first attempt to explain the graphite/salt composites behaviour. Int J Heat Mass Transf 2010;53:1195–207. doi:10.1016/j.ijheatmasstransfer.2009.10.025.
[29] Wu ZG, Zhao CY. Experimental investigations of porous materials in high temperature thermal energy storage systems. Sol Energy 2011;85:1371–80. doi:10.1016/j.solener.2011.03.021.
[30] Zhao CY, Wu ZG. Heat transfer enhancement of high temperature thermal energy storage using metal foams and expanded graphite. Sol Energy Mater Sol Cells 2011;95:636–43. doi:10.1016/j.solmat.2010.09.032.
[31] Yuan H-W, Lu C-H, Xu Z-Z, Ni Y-R, Lan X-H. Mechanical and thermal properties of cement composite graphite for solar thermal storage materials. Sol Energy 2012;86:3227–33. doi:10.1016/j.solener.2012.08.011.
[32] Li Y-F, Zhang D. Study on high-temperature phase change composites of NaNO3-LiNO3/expanded graphite by saturated water solution method. J Funct Mater 2013;44:1451–6.
[33] Xiao X, Zhang P, Li M. Thermal characterization of nitrates and nitrates/expanded graphite mixture phase change materials for solar energy storage. Energy Convers Manag 2013;73:86–94. doi:10.1016/j.enconman.2013.04.007.
[34] Huang Z, Gao X, Xu T, Fang Y, Zhang Z. Thermal property measurement and heat storage analysis of LiNO3/KCl – expanded graphite composite phase change material. Appl Energy 2014;115:265–71. doi:10.1016/j.apenergy.2013.11.019.
[35] Xiao J, Huang J, Zhu P, Wang C, Li X. Preparation, characterization and thermal properties of binary nitrate salts/expanded graphite as composite phase change material. Thermochim Acta 2014;587:52–8. doi:10.1016/j.tca.2014.04.021.
[36] Zhao YJ, Wang RZ, Wang LW, Yu N. Development of highly conductive KNO3/NaNO3 composite for TES (thermal energy storage). Energy 2014;70:272–7. doi:10.1016/j.energy.2014.03.127.
[37] Zhong L, Zhang X, Luan Y, Wang G, Feng Y, Feng D. Preparation and thermal properties of porous heterogeneous composite phase change materials based on molten salts/expanded graphite. Sol Energy 2014;107:63–73. doi:10.1016/j.solener.2014.05.019.

[38] Kim T, France DM, Yu W, Zhao W, Singh D. Heat transfer analysis of a latent heat thermal energy storage system using graphite foam for concentrated solar power. Sol Energy 2014;103:438–47. doi:10.1016/j.solener.2014.02.038.
[39] Zhao W, France DM, Yu W, Kim T, Singh D. Phase change material with graphite foam for applications in high-temperature latent heat storage systems of concentrated solar power plants. Renew Energy 2014;69:134–46. doi:10.1016/j.renene.2014.03.031.
[40] Lefebvre L-P, Banhart J, Dunand DC. Porous Metals and Metallic Foams: Current Status and Recent Developments. Adv Eng Mater 2008;10:775–87. doi:10.1002/adem.200800241.
[41] Chen J, Yang D, Jiang J, Ma A, Song D. Research Progress of Phase Change Materials (PCMs) Embedded with Metal Foam (a Review). Procedia Mater Sci 2014;4:389–94. doi:10.1016/j.mspro.2014.07.579.
[42] Yuan W, Tang Y, Yang X, Wan Z. Porous metal materials for polymer electrolyte membrane fuel cells – A review. Appl Energy 2012;94:309–29. doi:10.1016/j.apenergy.2012.01.073.
[43] Zhang P, Xiao X, Meng ZN, Li M. Heat transfer characteristics of a molten-salt thermal energy storage unit with and without heat transfer enhancement. Appl Energy 2015;137:758–72. doi:10.1016/j.apenergy.2014.10.004.
[44] Li Z, Wu Z-G. Numerical study on the thermal behavior of phase change materials (PCMs) embedded in porous metal matrix. Sol Energy 2014;99:172–84. doi:10.1016/j.solener.2013.11.017.
[45] Yang J, Du X, Yang L, Yang Y. Numerical analysis on the thermal behavior of high temperature latent heat thermal energy storage system. Sol Energy 2013;98, Part C:543–52. doi:10.1016/j.solener.2013.10.028.
[46] Yang J, Yang L, Xu C, Du X. Numerical analysis on thermal behavior of solid–liquid phase change within copper foam with varying porosity. Int J Heat Mass Transf 2015;84:1008–18. doi:10.1016/j.ijheatmasstransfer.2015.01.088.
[47] Choi SU., Eastman JA. Enhancing thermal conductivity of fluids with nanoparticles. Nternational Mech. Eng. Congr. Exhib., San Francisco, CA (United States): 1995.
[48] Al-Kayiem HH, Lin SC, Lukmon A. Review on nanomaterials for thermal energy storage technologies. Nanosci Nanotechnol-Asia 2013;3:60–71.
[49] Puliti G, Paolucci S, Sen M. Nanofluids and Their Properties. Appl Mech Rev 2011;64:1–24. doi:10.1115/1.4005492.
[50] Khanafer K, Vafai K. Chapter Five - Applications of Nanomaterials in Solar Energy and Desalination Sectors. In: Ephraim M. Sparrow YIC, John P. Abraham and John M. Gorman, editor. Adv. Heat Transf., vol. 45, Elsevier; 2013, p. 303–29.
[51] Khodadadi JM, Fan L, Babaei H. Thermal conductivity enhancement of nanostructure-based colloidal suspensions utilized as phase change materials for thermal energy storage: A review. Renew Sustain Energy Rev 2013;24:418–44. doi:10.1016/j.rser.2013.03.031.
[52] Xuan Y, Li Q. Heat transfer enhancement of nanofluids. Int J Heat Fluid Flow 2000;21:58–64. doi:10.1016/S0142-727X(99)00067-3.
[53] Saidur R, Leong KY, Mohammad HA. A review on applications and challenges of nanofluids. Renew Sustain Energy Rev 2011;15:1646–68. doi:10.1016/j.rser.2010.11.035.
[54] Raam Dheep G, Sreekumar A. Influence of nanomaterials on properties of latent heat solar thermal energy storage materials – A review. Energy Convers Manag 2014;83:133–48. doi:10.1016/j.enconman.2014.03.058.
[55] Kibria MA, Anisur MR, Mahfuz MH, Saidur R, Metselaar IHSC. A review on thermophysical properties of nanoparticle dispersed phase change materials. Energy Convers Manag 2015;95:69–89. doi:10.1016/j.enconman.2015.02.028.
[56] Andreu-Cabedo P, Mondragon R, Hernandez L, Martinez-Cuenca R, Cabedo L, Julia JE. Increment of specific heat capacity of solar salt with SiO2 nanoparticles. Nanoscale Res Lett 2014;9:1–11. doi:10.1186/1556-276X-9-582.
[57] Shin D, Banerjee D. Enhancement of specific heat capacity of high-temperature silica-nanofluids synthesized in alkali chloride salt eutectics for solar thermal-energy storage applications. Int J Heat Mass Transf 2011;54:1064–70. doi:10.1016/j.ijheatmasstransfer.2010.11.017.

[58] Ho MX, Pan C. Optimal concentration of alumina nanoparticles in molten Hitec salt to maximize its specific heat capacity. Int J Heat Mass Transf 2014;70:174–84. doi:10.1016/j.ijheatmasstransfer.2013.10.078.
[59] Siegel R. Solidification of low conductivity material containing dispersed high conductivity particles. Int J Heat Mass Transf 1977;20:1087–9. doi:10.1016/0017-9310(77)90195-8.
[60] Keblinski P, Phillpot SR, Choi SUS, Eastman JA. Mechanisms of heat flow in suspensions of nano-sized particles (nanofluids). Int J Heat Mass Transf 2002;45:855–63. doi:10.1016/S0017-9310(01)00175-2.
[61] Koo J, Kleinstreuer C. A new thermal conductivity model for nanofluids. J Nanoparticle Res 2005;6:577–88. doi:10.1007/s11051-004-3170-5.
[62] Jang SP, Choi SUS. Role of Brownian motion in the enhanced thermal conductivity of nanofluids. Appl Phys Lett 2004;84:4316–8. doi:10.1063/1.1756684.
[63] Yu W, France DM, Routbort JL, Choi SUS. Review and Comparison of Nanofluid Thermal Conductivity and Heat Transfer Enhancements. Heat Transf Eng 2008;29:432–60. doi:10.1080/01457630701850851.
[64] Dudda B, Shin D. Effect of nanoparticle dispersion on specific heat capacity of a binary nitrate salt eutectic for concentrated solar power applications. Int J Therm Sci 2013;69:37–42. doi:10.1016/j.ijthermalsci.2013.02.003.
[65] Shi Y, Yuan HW, Xu ZZ, Lu CH, Ni YR, Dong Y. Thermal and Mechanical Properties of Aluminate Cementitious Functional Materials Enriched with Nano-SiO2 for Thermal Energy Storage. Adv Mater Res 2014;887-888:77–80. doi:10.4028/www.scientific.net/AMR.887-888.77.
[66] Yuan H, Shi Y, Xu Z, Lu C, Ni Y, Lan X. Influence of nano-ZrO2 on the mechanical and thermal properties of high temperature cementitious thermal energy storage materials. Constr Build Mater 2013;48:6–10. doi:10.1016/j.conbuildmat.2013.06.088.
[67] Yuan H, Shi Y, Xu Z, Lu C, Ni Y, Lan X. Effect of nano-MgO on thermal and mechanical properties of aluminate cement composite thermal energy storage materials. Ceram Int 2014;40:4811–7. doi:10.1016/j.ceramint.2013.09.030.
[68] Yuan H, Shi Y, Lu C, Xu Z, Ni Y, Lan X. Enhanced performance of high temperature aluminate cementitious materials incorporated with Cu powders for thermal energy storage. Cem Concr Compos 2015;55:139–44. doi:10.1016/j.cemconcomp.2014.08.006.
[69] Liu M, Ma Y, Wu H, Wang RY. Metal matrix-metal nanoparticle composites with tunable melting temperature and high thermal conductivity for phase-change thermal storage. ACS Nano 2015;9:1341–51. doi:10.1021/nn505328j.
[70] Shin D, Banerjee D. Enhanced thermal properties of SiO2 nanocomposite for solar thermal energy storage applications. Int J Heat Mass Transf 2015;84:898–902. doi:10.1016/j.ijheatmasstransfer.2015.01.100.
[71] Ye F, Ge Z, Ding Y, Yang J. Multi-walled carbon nanotubes added to Na2CO3/MgO composites for thermal energy storage. Particuology 2014;15:56–60. doi:10.1016/j.partic.2013.05.001.
[72] Tao YB, Lin CH, He YL. Preparation and thermal properties characterization of carbonate salt/carbon nanomaterial composite phase change material. Energy Convers Manag 2015;97:103–10. doi:10.1016/j.enconman.2015.03.051.
[73] Cingarapu S, Singh D, Timofeeva EV, Moravek MR. Nanofluids with encapsulated tin nanoparticles for advanced heat transfer and thermal energy storage. Int J Energy Res 2014;38:51–9. doi:10.1002/er.3041.
[74] Timofeeva EV, Moravek MR, Singh D. Improving the heat transfer efficiency of synthetic oil with silica nanoparticles. J Colloid Interface Sci 2011;364:71–9. doi:10.1016/j.jcis.2011.08.004.
[75] Mankins JC. Technology readiness levels. NASA 1995. http://www.hq.nasa.gov/office/codeq/trl/trl.pdf (accessed March 31, 2015).
[76] European Comission. Technology readiness levels (TRL). Horiz 2020 – WORK Programme 2014 - 2015 Gen Annex 2014. http://ec.europa.eu/research/participants/data/ref/h2020/wp/2014_2015/annexes/h2020-wp1415-annex-g-trl_en.pdf (accessed March 31, 2015).

[77] Ibáñez JM. Niveles de madurez de la tecnología. Technology readiness levels. TRLs. Una introducción. Minist Indústria Energ Tur 2014. http://www.minetur.gob.es/Publicaciones/Publicacionesperiodicas/EconomiaIndustrial/RevistaEconomiaIndustrial/393/NOTAS.pdf (accessed March 31, 2015).